NASA Technical Paper 1632

Supersonic Wings With Significant Leading-Edge Thrust at Cruise

A. Warner Robins, Harry W. Carlson,
and Robert J. Mack

APRIL 1980

NASA

NASA Technical Paper 1632

Supersonic Wings With Significant Leading-Edge Thrust at Cruise

A. Warner Robins, Harry W. Carlson,
and Robert J. Mack
Langley Research Center
Hampton, Virginia

National Aeronautics
and Space Administration

**Scientific and Technical
Information Office**

1980

SUMMARY

Experimental/theoretical correlations are presented which show that significant levels of leading-edge thrust are possible at supersonic speeds for certain planforms having the geometry to support the theoretical thrust-distribution potential. The new analytical process employed provides not only the level of leading-edge thrust attainable but also the spanwise distribution of both it and that component of full theoretical thrust which acts as vortex lift. Significantly improved aerodynamic performance in the moderate supersonic speed regime is indicated.

INTRODUCTION

Aerodynamicists have long known of the importance of leading-edge thrust to the performance of subsonic airplanes. These forces, which arise from the very low pressures induced by the high velocities of the flow around the leading edge from a stagnation point beneath the wing, largely counteract the drag from the remainder of the airfoil in high-aspect-ratio wings at low speeds. Efforts to extend these benefits to the higher speeds have led to the swept wings commonly seen in present-day, long-range airplanes. Indeed, according to theory, should wing leading edges be swept sufficiently behind the Mach line, there is a theoretical potential for leading-edge thrust at supersonic speeds. Although some evidence of the attainment of this thurst force has been shown at supersonic speeds (for example, ref. 1), it was believed to occur to an appreciable extent only for wings with geometric characteristics unsuitable for supersonic cruise. Thus, thrust effects at supersonic speeds for vehicles designed for supersonic cruise have generally been ignored in supersonic aerodynamic design and analysis.

It has been common practice to optimize wing lifting efficiency at supersonic speeds through the use of wing surface shaping which at the lift coefficient for the design of that camber surface precludes attainment of any leading-edge thrust. The resultant camber surfaces for full theoretical benefits, however, may be too severe for incorporation into practical airplane designs. The large root chord angle and the resultant large cabin floor angle are particularly troublesome. Furthermore, the severe camber surfaces may violate the small-disturbance assumptions of the linearized theory on which the wing design is based, and the full theoretical benefits of twist and camber are seldom, if ever, achieved. In fact, design lift coefficients for supersonic wing-surface optimization are almost always lower than the lift coefficient for maximum lift-drag ratio in order to meet practical geometric restraints and to avoid the point of diminishing aerodynamic returns. If it were possible to attain nearly full theoretical leading-edge thrust over even a limited additional lift-coefficient range, performance levels approaching the full theoretical twist and camber levels could be achieved with wings of moderate camber-surface severity.

A recent experimental investigation (ref. 2) has in fact demonstrated a substantial degree of leading-edge thrust at supersonic speeds for a wing having a novel planform shape. It is the purpose of this paper to analyze these results in order to understand the cause of the unexpected performance benefit and to develop a design rationale for further exploitation of the thrust phenomena as applied to supersonic cruise vehicles. For that purpose, recently developed analytical methods for the estimation of full theoretical thrust and attainable thrust have been employed. It is shown that certain planforms favor the development of leading-edge thrust, that significant amounts of leading-edge thrust can be achieved for wings suitable for supersonic cruise, and that a new method for prediction of attainable thrust makes possible a rational design process for exploiting this potential gain in cruise aerodynamic performance.

SYMBOLS

b	wing span
c	wing chord length
$\bar{c}$	mean aerodynamic chord
C_D	drag coefficient
C_L	lift coefficient
C_m	pitching-moment coefficient
C_A	axial- or chord-force coefficient
C_p	pressure coefficient
C_t	local thrust coefficient
C_T	total thrust coefficient, $2\int_0^{b/2} C_t \, dy$
L/D	lift-drag ratio, C_L/C_D
M	free-stream Mach number
R	free-stream Reynolds number
t	maximum thickness of local wing chord
x	longitudinal distance to local wing leading edge
y	spanwise distance from plane of symmetry
α	angle of attack, deg

β $= \sqrt{M^2 - 1}$

Λ local leading-edge sweep angle, deg

Subscripts:

$\bar{c}$ referenced to mean aerodynamic chord

l limiting condition

n pertaining to wing section normal to leading edge

max maximum value

DISCUSSION

Experimental/Theoretical Considerations

A comparison of the experimental and theoretical drag polars of three slender supersonic-cruise configurations is shown in figure 1. The two on the left, which were tested at a Mach number of 2.7, were the last competing pair in the national SST program. The configuration on the right, which is a NASA concept (ref. 3) of essentially the same vintage, was tested at a Mach number of 2.6. All were tested in the Langley Unitary Plan Wind Tunnel at a Reynolds number, based on mean aerodynamic chord, of approximately 5×10^6.

All three configurations have subsonic leading edges over much of the wing span (that is, local leading edge swept behind the Mach line). The generally good agreement between calculation (refs. 4, 5, and 6) and experiment in which measured drag generally exceeds theory by small amounts, if any, would suggest some validity in the usually accepted assumption of no leading-edge thrust in the calculation methods. These data are characteristic of supersonic drag polars at design speed, generally. Thus, as mentioned previously, supersonic design and evaluation methods have generally (and, perhaps, conveniently) neglected leading-edge thrust.

Some insight into the lack of attainment of significant amounts of leading-edge thrust at cruise for supersonic-cruise configurations may be gained from figure 2. Here theoretical maximum thrust (ref. 7) and bluntness or thickness comparisons are shown (with thickness somewhat exaggerated for clarity) for two planforms having predominantly subsonic leading edges. For the more conventional straight-leading-edge wing, where there is potential for thurst, there is little thickness or bluntness for the attainable pressures to act upon. The complex-leading-edge wing, however, with its higher inboard sweep (reaching almost 80°) and fuller inboard thickness, shows a significant thrust potential where the geometry favors its attainment. Put another way, there is upwash where there is thickness. Comparisons of experimental and theoretical static longitudinal aerodynamic characteristics of a wing model having the planform of this complex wing are shown subsequently.

The model (ref. 2) had a design Mach number of 1.8, a design lift coefficient of 0.07, and NACA 65A004 airfoil sections and was essentially a wing alone, having a small balance housing mounted essentially symmetrically about the camber plane and faired smoothly into the forward surfaces of the wing. As shown in figure 3, tests were conducted at the design Mach number of 1.8 and at a Reynolds number based on mean aerodynamic chord of 2.07×10^6. The theoretical data were obtained through use of a computing program described in references 8, 9, and 10. This program provides estimates of aerodynamic performance based on numerical solutions of linearized-theory integral equations. As an option, the program provides performance estimates for the case where local pressures are limited to some fraction of the vacuum pressure (in this case, 0.75). Theoretical leading-edge-thrust estimates were obtained from a computing program described in reference 7. The estimate of vortex lift - a subject extensively treated in reference 11 - was obtained by using the Polhamus leading-edge-suction analogy (ref. 12), and applying it to the leading-edge-thrust estimate. The thrust or vortex increments were added vectorially to the results from the basic linearized-theory computing program, neglecting the additional $\sin \alpha$ and $\cos \alpha$ surface-boundary-condition terms employed in reference 12, since the calculations were limited to small angles of attack. Compare first the experimental data with the no-leading-edge-thrust linear theory without pressure-coefficient limiting or consideration of vortex lift. The experimental nonlinearities in the lift curve and in the pitching moment, in particular, are not represented by theory, nor is there adequate representation of lift-drag ratio at optimum lift (lift coefficient for maximum lift-drag ratio). Arbitrarily limiting the linear-theory pressure coefficients (which might otherwise be below vacuum) to 3/4 vacuum results in the dashed curves. Breaks are now seen in the theory curves which would seem to result from significant and progressive lift losses from the tip region inboard, as indicated by the severity of the pitching-moment nonlinearity. Thus, it would seem that theory without pressure constraint calls for potential flow pressures which physically cannot be achieved. Some other flow mechanism must therefore have existed. Assuming that, when potential flow cannot be fully maintained, the Polhamus vortex-lift analogy (ref. 12) applies, normal-force increments representing the effects of the leading-edge separated vortex flow were then applied to the limited linear-theory values. The resulting theoretical values are seen in figure 3 as the long-dash—short-dash curve. This method (limited linear theory with vortex lift), all parameters considered, is certainly an improvement, but there remains a large discrepancy in maximum lift-drag ratio beyond that which might have arisen from the 0.00044 increment by which theory overpredicts zero-lift drag coefficient (see ref. 2).

On the assumption that prior to manifesting itself as vortex lift, some leading-edge thrust might, indeed, have occurred, the curve showing the pressure-coefficient-limited linear theory without vortex lift but with full theoretical thrust is presented. Agreement at maximum lift-drag ratio is much improved. There remains, however, a problem beyond predicting leading-edge thrust or vortex lift at supersonic speeds, and that is the analytical representation of the transition from the full thrusting mode to the full vortex-lift mode.

New Analytical Method

A new method (ref. 13) for estimation of attainable thrust has been developed and the key features thereof are presented in figure 4. The method applies simple sweep theory to wings of arbitrary planform to permit two-dimensional analysis. A comprehensive survey of two-dimensional data is correlated to provide limiting-pressure restraints as a function of these normal Mach and Reynolds numbers. Correlation equations derived from theoretical two-dimensional data then provide thrust-coefficient limitation as a function of theoretical thrust, empirically limited pressure, and airfoil section parameters. With these relationships programmed as a subroutine in existing lifting-surface programs, spanwise distribution of attainable thrust (which might contain a component of vortex lift) is directly available for use in lift and drag estimation. These lift and drag relationships are compatible with the Polhamus leading-edge-suction analogy for fully detached leading-edge flow with vortex-induced reattachment when the analogy is taken to be the limiting case of a gradual rotation of the full suction vector as leading-edge thrust is lost. Thus, the method does provide a rational analytical means for making the transition from the full thrust mode to that of full vortex lift.

In figure 5, which continues consideration of the complex configuration of figure 2, experimental axial-force coefficient - a parameter sensitive to leading-edge thrust - is compared over the lift range with theoretical values for full leading-edge thrust and no leading-edge thrust, as well as for attainable thrust from the new method (ref. 13). The previously mentioned increment in drag is removed so that experiment and theory coincide at the design lift coefficient (0.07). In addition to the basic curve containing the axial-force component of both the attainable leading-edge thrust and attainable vortex-lift vectors, a curve containing only the attainable-thrust component is shown. The favorable and unfavorable vortex-lift increments between these two curves at positive and negative lifts, respectively, are unrealistically large because the method of calculation contains the assumption that the vortex-lift vector is applied normal to the camber surface right at the leading edge where surface slope is greatest. Newer techniques provide for application farther back on the surface so as to be more in keeping with actual flow physics. The main point of this figure, however, is to show that not only is a significant amount of experimental leading-edge thrust indicated, but a reasonably good representation of experiment by the new method is obtained in the positive-lift range up to lift coefficients of approximately 0.3.

Returning to the lift-drag-ratio comparisons between theory and experiment, the attainable curve in figure 6 is seen to agree with the full-thrust values in a very limited low-lift range. From the low lift-coefficient values of such agreement to the highest values shown, the new method provides that less and less of the leading-edge force be manifested as thrust, and more and more be manifested as vortex lift. The inset flow-visualization photographs, taken at the conditions represented by the solid symbols, are included to provide an understanding of the flow physics at those points. The upper pair of photographs are of the upper surfaces of the model with a fluorescent oil coating, which, under the action of the flow, has essentially stabilized at each of the two conditions. The picture at the right is taken from above the right rear quadrant of the model as it is immersed in humid, partially condensed flow and

illuminated by a thin fan of intense light positioned normal to the flow. Strong vortices appear at this high-lift condition as the pair of dark circles located above the wing surface about midway between the wing leading edges and the model plane of symmetry. Thus, the upper-surface flow appears to vary from the classic potential-flow condition at the lift coefficient for which the wing camber was designed, through a condition in which there is a mixed flow including some vorticity, to the condition at high lifts in which there is upper-surface vortex flow without reattachment. In any event, the modified linear theory method of reference 13, which attempts to account for these nonlinear types of flow, provides, in addition to an indication of significant amounts of leading-edge thrust, a substantially improved representation of the experimental results. Note for future reference that angles of attack of 2° and 4° fall just below and above that for maximum lift-drag ratio.

Spanwise Distribution of Thrust

With supersonic thrust distribution being so critically dependent upon the degree to which the leading edge is swept behind the Mach line, consideration of the spanwise distribution of thrust in figure 7 begins with the spanwise distribution of a parameter $1/(\beta \cot \Lambda)$ which is the ratio of the tangent of the leading-edge sweep angle to the tangent of the sweep of the Mach line. Thus, the higher the values of $1/(\beta \cot \Lambda)$, the more subsonic the leading edge is, with the value of unity representing a sonic leading edge and lesser values corresponding to a supersonic leading edge. The calculated (ref. 13) values of local thrust coefficient for the experimental configuration at test Reynolds number (2.07×10^6) and at design Mach number (1.8) are shown divided by α^2. This is a convenient way to express local thrust, since theoretical maximum thrust coefficient is a direct function of α^2 and the aim here is to show that as angle of attack is increased the portion of maximum theoretical thrust which appears to be attainable becomes smaller. It should be recalled that the theory assumes that attainable thrust is that component of maximum theoretical thrust which manifests itself as thrust, while the normal component of that theoretical maximum manifests itself as vortex lift, with the difference between the $C_{t,max}$ and C_t curves defining the location and intensity of the latter. Thus, theoretically, the loss of thrust and the attendant development of vortex lift begins outboard and moves progressively inboard as angle of attack is increased. This analytical degradation in percent of maximum theoretical thrust and the corresponding increase in vortex lift as angle of attack is increased from 2° to 4° in this figure correspond to the lift-drag-ratio decrements between full and attainable thrust at these two angles in figure 6. The calculated values of both figures 6 and 7 indicate the effect of considerable vorticity at the higher angle (4°), with the former (fig. 6) providing strong experimental evidence in the corresponding oil-flow photograph.

To prevent an assumption that attainable thrust decreases with increasing angle of attack, the remaining thrust-distribution figures, beginning with figure 8, deal in absolute values of calculated local thrust coefficient at the two angles of attack of 2° and 4°. In fact, these figures show that calculated attainable thrust at 4° exceeds, in most cases, the theoretical maximum thrust at an angle of attack of 2°.

The calculated values of absolute local thrust coefficients in figure 8 are for the same conditions as in figure 7, except that values for a full-scale Reynolds number of 128×10^6 (corresponding to $c = 25.3$ m and an altitude of 17 400 m) have been added. For convenience, the value of total thrust coefficient C_T, which is twice the integral of the local coefficients, is shown for each Reynolds number. At an angle of attack of 2^o, thrust loss begins near mid-semispan and there is approximately a count (0.0001) difference in the total thrust coefficients for Reynolds numbers of 2.07×10^6 and 128×10^6, with the value for 128×10^6 being about two counts less than the theoretical maximum value (for $R = \infty$). At 4^o, however, there is an appreciable difference in location of thrust loss and nearly five counts difference between tunnel and full-scale Reynolds number, with that for the latter being approximately half the 34-count theoretical maximum value. In this case, the effects of Reynolds number on thrust are seen to be important, but certainly not critical.

The local thrust coefficient values of figure 9 are for the same basic configuration at a Reynolds number of 128×10^6, but with another Mach number of 1.4 as well as the original 1.8. Although the spanwise location of thrust loss here does not appear to be strongly dependent on Mach number, both the attainable (ref. 13) and the theoretical maximum values of total thrust appear to be very much so. At both angles of attack, attainable thrust at a Mach number of 1.4 is about double that at a Mach number of 1.8, with some 35 1/2 counts appearing to be attainable out of the 65 counts of theoretical maximum thrust at $M = 1.4$ and $\alpha = 4^o$. Because of the importance of the leading-edge-sweep parameter in determination of wing aerodynamic performance, this result suggests that improved thrust may be obtained at the original Mach number of 1.8 by increasing the sweep angle to provide a distribution of $1/(\beta \cot \Lambda)$ equal to that of the original wing at $M = 1.4$. Further considerations of the leading-edge-sweep parameter in selection of wing planforms which favor the attainment of leading-edge thrust and the attendant performance benefits are discussed in a subsequent section.

In figure 10, calculated (ref. 13) local thrust coefficients for a Mach number of 1.8 and a Reynolds number of 128×10^6 are shown for the basic configuration with its 4-percent-thick wing, and for variations in wing thickness to 3 and 5 percent. Qualitatively, the inboard progression of thrust loss with decreasing thickness is as would be expected. As was the case for Reynolds number variation in figure 8, the effect of the present variable (t/c) is seen, within the range shown (0.03 to 0.05), to be important to leading-edge thrust, but certainly not critical.

Thrust-Dependent Lift-Drag Ratio

The calculated thrust distributions (figs. 8, 9, and 10) have shown, for the basic study configuration and variations thereof, the dependence of leading-edge thrust on Reynolds number, Mach number, and thickness ratio. Figure 11 addresses the effects of these same three variables (R, M, and t/c) on maximum lift-drag ratio, including leading-edge thrust effects. In each case, the theoretical curves for full leading-edge thrust, no leading-edge thrust, and attainable thrust are shown. Where available, the appropriate experimental

points are presented. Unless otherwise indicated on an abscissa, Mach number is 1.8 and thickness ratio is 0.04.

The large effect on maximum lift-drag ratio of the variation of Reynolds number is almost entirely that due to the change in viscous drag. Calculated attainable thrust is seen to vary from about half the increment between no thrust and full thrust at the lowest Reynolds number to about 60 percent at the highest - a small amount compared with that due to the viscous-drag change. The agreement between experiment and calculation seems reasonably good.

The effect on maximum lift-drag ratio of varying Mach number over the range shown is particularly large for the full-thrust case at both the test and full-scale Reynolds numbers, with the attainable-thrust curve showing a similarly large variation at the high Reynolds number. In contrast, the attainable-thrust variation at test Reynolds number (2.07×10^6) falls about midway between the full-thrust values and those for the relatively insensitive no-thrust curve. This greater thrust dependency on Mach number certainly suggests that in the extrapolations of such wind-tunnel data to full-scale conditions care should be taken to account for leading-edge thrust. Again, agreement between experiment and calculation is reasonably good, but particularly significant to the designer is that agreement at the $M = 1.5$ condition, for it suggests that very high values of $1/(\beta \cot \Lambda)$ (or very low Mach number components normal to the wing leading edge) may be employed without incurring fully separated flow conditions.

The sharp variations of maximum lift-drag ratio with thickness ratio are again seen to be an effect of minimum drag. Here, it is a large variation of zero-lift wave drag with thickness. The steeper variation at the full-scale Reynolds number is due to the combining of the additional viscous-drag decrement with the sharply changing wave drag to produce, as thickness is reduced, very low values of minimum drag and consequently high lift-drag ratios. An interesting additional point is that, at full-scale Reynolds number, values of maximum lift-drag ratio corresponding to the attainable-thrust curve did not sharply fall off toward the no-thrust curve as thickness decreased.

It has been noted that supersonic-cruise designs have generally been based on analytical methods which excluded leading-edge thrust and thus correspond to the dashed-curve values of figure 11. However, as has been seen here, significant amounts of leading-edge thrust can be generated for a certain class of supersonic wings. Furthermore, as indicated by the analytical and experimental data shown here, these benefits are surprisingly tolerant of high values of $1/(\beta \cot \Lambda)$ (lower Mach numbers in this case), where, particularly for thin wings, early onset of fully separated flow might have been expected. Thus, very high levels of supersonic aerodynamic performance seem possible.

Returning to the spanwise variation of the design parameter $1/(\beta \cot \Lambda)$, upon which leading-edge thrust is so dependent - in figure 12 a curve corresponding to the basic configuration at a Mach number of 1.5, the dashed line in the left portion of the figure, is compared with the curve for the basic configuration at the design Mach number 1.8 (taken from fig. 7). It is this much more subsonic leading-edge condition which appears to have worked well at $M = 1.5$ (see fig. 11). The leading edge of a new wing with a design Mach number of 1.8,

but with the same spanwise schedule of $1/(\beta \cot \Lambda)$ as the original configuration A at $M = 1.5$, is defined by the indicated integration of the dashed curve. A further perturbation which would depart from configuration B by trading toward a lower sweep, shorter outboard panel and to a lower thickness (3 percent) is shown on the right in figure 12 as configuration C. Here the rationale was to forego thrust on the outboard panel, where attainable thrust tends to be small and sensitive to angle of attack, and to achieve lower zero-lift wave drag. Note that all wings shown have the same wing area and tip chord.

Calculated maximum lift-drag ratio and the product of it and Mach number are shown for 4-percent-thick versions of wings A and B at Mach numbers 1.5 and 1.8 and at test and full-scale Reynolds numbers in figure 13. The available corresponding experimental values are also shown as circular symbols. At full-scale Reynolds number, both $(L/D)_{max}$ and $M(L/D)_{max}$ are higher for wing B at $M = 1.8$ than for wing A at either Mach number. Configuration B is such, however, that severe structural or low-speed longitudinal-stability problems might be encountered. The somewhat more practical configuration C, the simple variation of configuration B, is seen to outperform both A and B. Further perturbations should produce even better results. There remains, however, a need for further experimental verification.

Additional Design Considerations

A broader view of wings designed to operate at cruise with a significant amount of leading-edge thrust allows several design-oriented observations to be made with the aid of figure 14. In this figure, the planform of the present study is shown shaded and superimposed on the containing delta planform. Recognizing the seeming inevitable shrinkage in wing size (to reduce wetted area and weight) in the successive stages of design cycling from the initial concept, the lower half of the planform figure was prepared to show the containing delta and a shrunken version thereof having the same planform area as the shaded part of the upper half. Immediately apparent is its much-reduced effective lifting length and shorter span compared with the initial shaded planform. Considering that supersonic drag due to lift is an inverse function of the combination of the square of the lifting length and the square of the span (see ref. 14), it is critically important to aerodynamic performance to be particularly selective in reducing wing area. The shaded planform reduces wing area but preserves the overall length and span, and thus should tend to retain the aerodynamic efficiency of the containing delta. Another point regarding the shaded planform is that structurally it should tend to resemble a wing having the planform represented by the shaded area rearward of the short-dash line, but to which has been added a forward strake.

A final point to be made through this figure is in regard to treatment of the planform at the wing tip. It is suggested that the wing outer panel be tailored to provide that vortex flow initiate along the leading edge, providing not only for its suction effect on the upper surface, but for a vortex-induced flow reattachment and its scavenging effect over the tip area which might otherwise experience flow separation as in the inset sketch at the bottom of the figure.

CONCLUDING REMARKS

There are several observations growing out of the present study which should be of interest to the designer of supersonic-cruise vehicles. Foremost is that experimental results indicate the presence of significant amounts of leading-edge thrust at supersonic speeds. Furthermore, there is a new methodology for the prediction of attainable leading-edge thrust and/or that component of thrust which acts as vortex lift. There is, as well, a new class of supersonic wings which matches the theoretical thrust-distribution potential with supporting airfoil geometry (that is, which places upwash where there is bluntness). These wings should lead to higher maximum lift-drag ratios at higher lift coefficients. Noting that with the attainment of substantial amounts of leading-edge thrust at supersonic speeds increasing with diminishing Mach numbers, efforts to significantly improve airplane range should give rise to serious consideration of lower supersonic-cruise speeds (of the order of a Mach number of 2 or less). These lower speeds should offer more speed-compatible airframes and propulsion systems.

Langley Research Center
National Aeronautics and Space Administration
Hampton, VA 23665
March 7, 1980

REFERENCES

1. Polhamus, Edward C.: Drag Due to Lift at Mach Numbers up to 2.0. NACA RM L53I22b, 1953.

2. Robins, A. Warner; Lamb, Milton; and Miller, David S.: Aerodynamic Characteristics at Mach Numbers of 1.5, 1.8, and 2.0 of a Blended Wing-Body Configuration With and Without Integral Canards. NASA TP-1427, 1979.

3. Morris, Odell A.; and Fournier, Roger H.: Aerodynamic Characteristics at Mach Numbers 2.30, 2.60, and 2.96 of a Supersonic Transport Model Having a Fixed, Warped Wing. NASA TM X-1115, 1965.

4. Harris, Roy V., Jr.: An Analysis and Correlation of Aircraft Wave Drag. NASA TM X-947, 1964.

5. Middleton, Wilbur D.; and Carlson, Harry W.: Numerical Method of Estimating and Optimizing Supersonic Aerodynamic Characteristics of Arbitrary Planform Wings. J. Aircr., vol. 2, no. 4, July-Aug., 1965, pp. 261-265.

6. Sommer, Simon C.; and Short, Barbara J.: Free-Flight Measurements of Turbulent-Boundary-Layer Skin Friction in the Presence of Severe Aerodynamic Heating at Mach Numbers From 2.8 to 7.0. NACA TN 3391, 1955.

7. Carlson, Harry W.; and Mack, Robert J.: Estimation of Leading-Edge Thrust for Supersonic Wings of Arbitrary Planform. NASA TP-1270, 1978.

8. Middleton, W. D., and Lundry, J. L.: A Computational System for Aerodynamic Design and Analysis of Supersonic Aircraft. Part 1 - General Description and Theoretical Development. NASA CR-2715, 1976.

9. Middleton, W. D.; Lundry, J. L.; and Coleman, R. G.: A Computational System for Aerodynamic Design and Analysis of Supersonic Aircraft. Part 2 - User's Manual. NASA CR-2716, 1976.

10. Middleton, W. D.; Lundry, J. L.; and Coleman, R. G.: A Computational System for Aerodynamic Design and Analysis of Supersonic Aircraft. Part 3 - Computer Program Description. NASA CR-2717, 1976.

11. Kulfan, R. M.: Wing Geometry Effects on Leading-Edge Vortices. AIAA Paper 79-1872, Aug. 1979.

12. Polhamus, Edward C.: Predictions of Vortex-Lift Characteristics by a Leading-Edge Suction Analogy. J. Aircr., vol. 8, no. 4, Apr. 1971, pp. 193-199.

13. Carlson, Harry W.; Mack, Robert J.; and Barger, Raymond L.: Estimation of Attainable Leading-Edge Thrust for Wings at Subsonic and Supersonic Speeds. NASA TP-1500, 1979.

14. Goldsmith, H. A.: Supersonic Transports. Advancing Technologies, E. G. Semler, ed., Mechanical Engineering Publ., Ltd., c.1977, pp. 10-24.

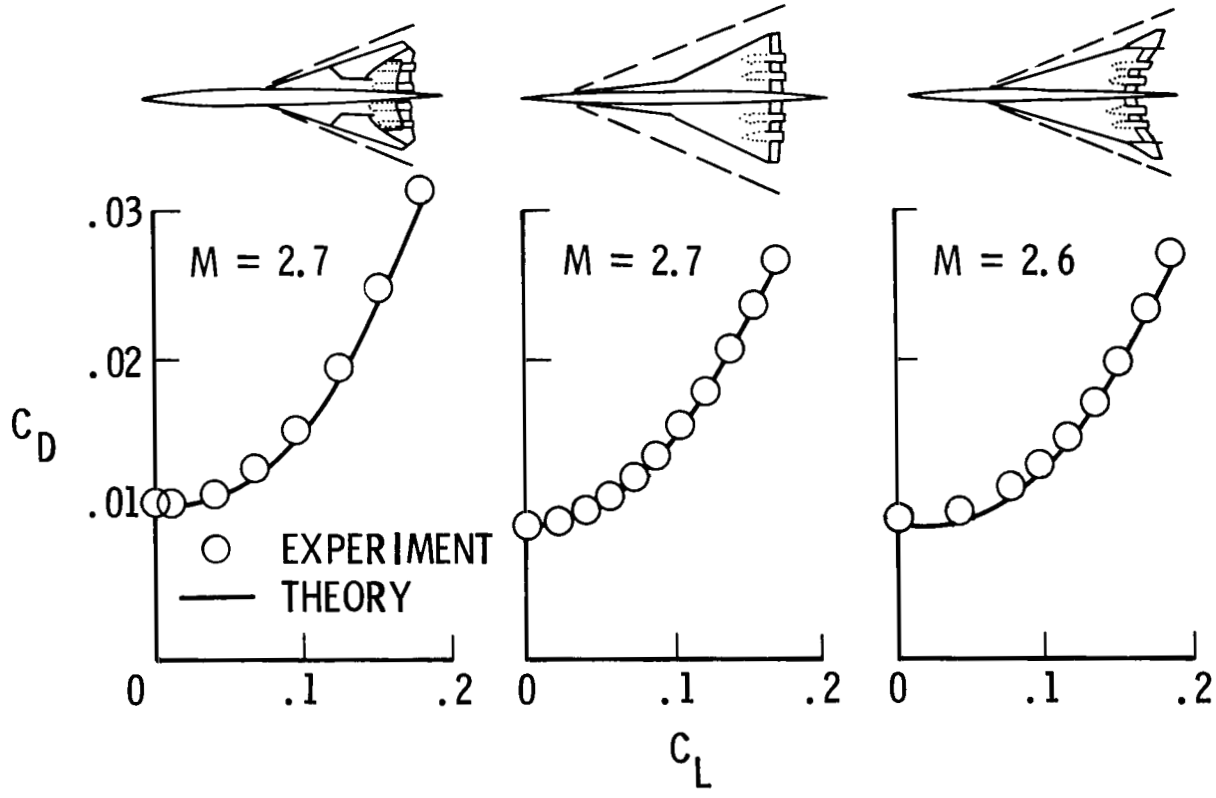

Figure 1.- Experimental and theoretical drag polars of models of supersonic-cruise airplanes. $R_{\bar{c}} \approx 4.8 \times 10^6$.

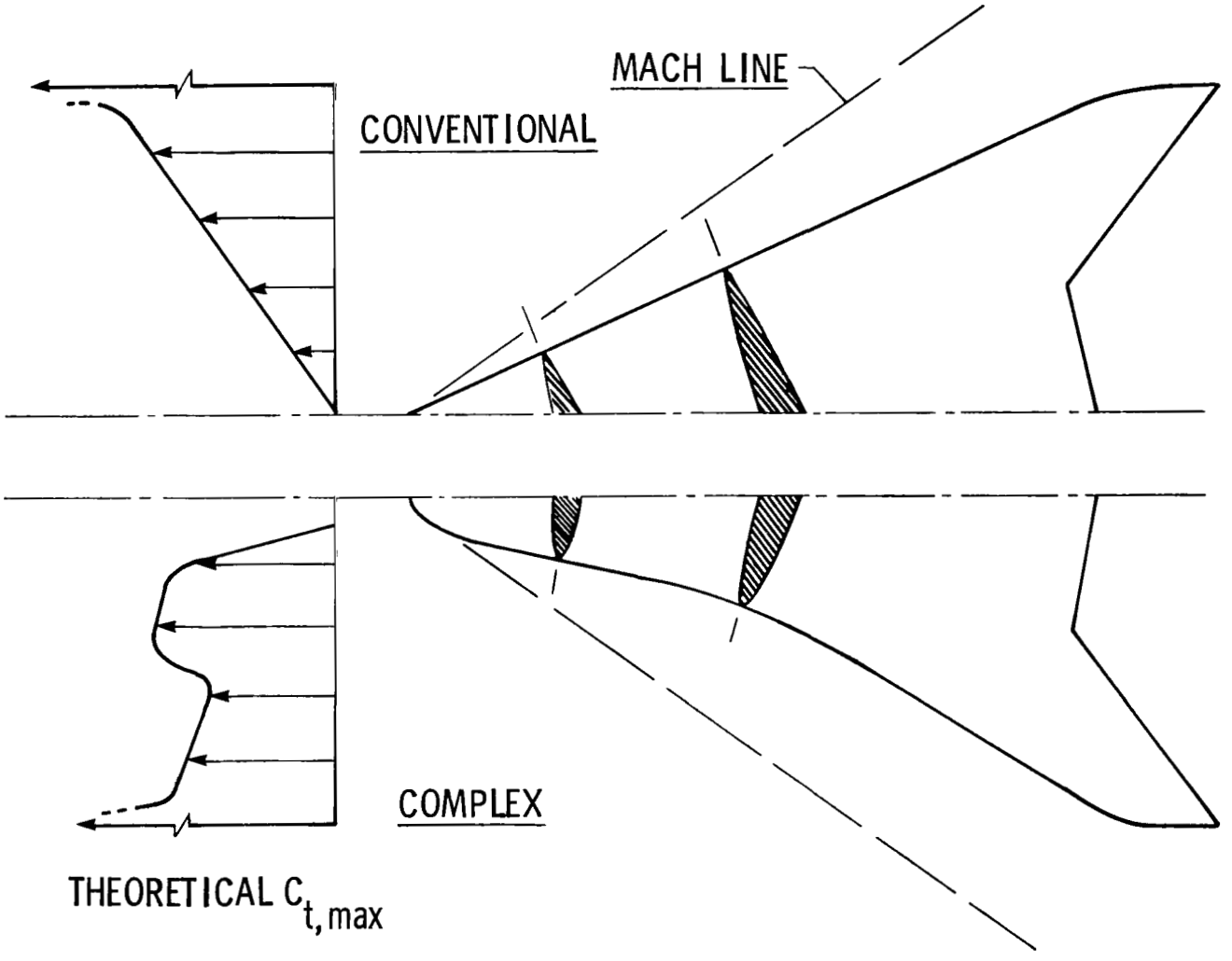

Figure 2.- Thrust and thickness comparisons near wing leading edge.

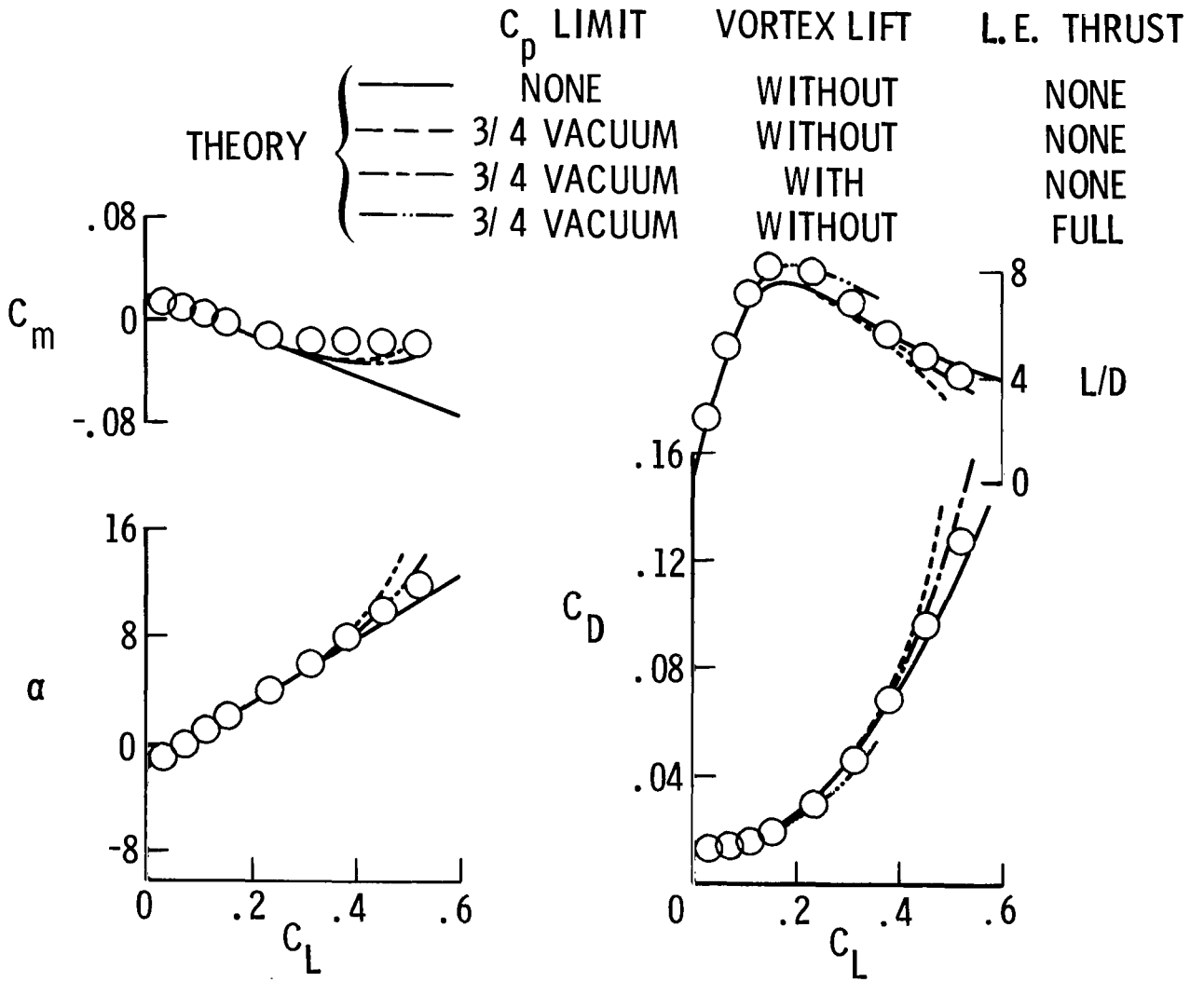

Figure 3.- Experimental and theoretical static longitudinal aerodynamic characteristics. $M = 1.8$; $R_{\bar{c}} = 2.07 \times 10^6$.

APPLICATION OF SIMPLE SWEEP THEORY

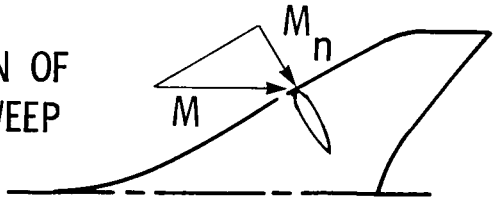

TO WINGS OF ARBITRARY PLANFORM PERMITS TWO-DIMENSIONAL ANALYSIS

EXPERIMENTAL TWO-DIMENSIONAL DATA PROVIDE LIMITING PRESSURE RESTRAINTS

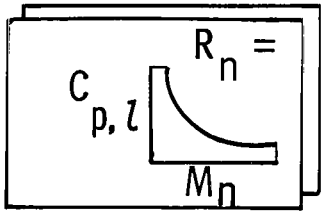

AS A FUNCTION OF MACH NUMBER AND REYNOLDS NUMBER

THEORETICAL TWO-DIMENSIONAL DATA PROVIDE THRUST COEFFICIENT LIMITATION

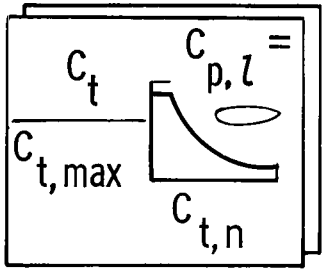

AS A FUNCTION OF THEORETICAL THRUST, LIMITING PRESSURE, AND AIRFOIL SECTION PARAMETERS

ABOVE RELATIONSHIPS PROGRAMMED AS A SUBROUTINE IN LIFTING SURFACE PROGRAMS PROVIDE SPANWISE THRUST DISTRIBUTIONS

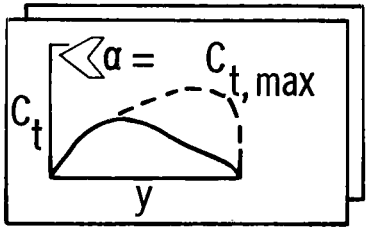

FOR USE IN AERODYNAMIC PERFORMANCE ESTIMATES

Figure 4.- Key features of attainable-thrust prediction method.

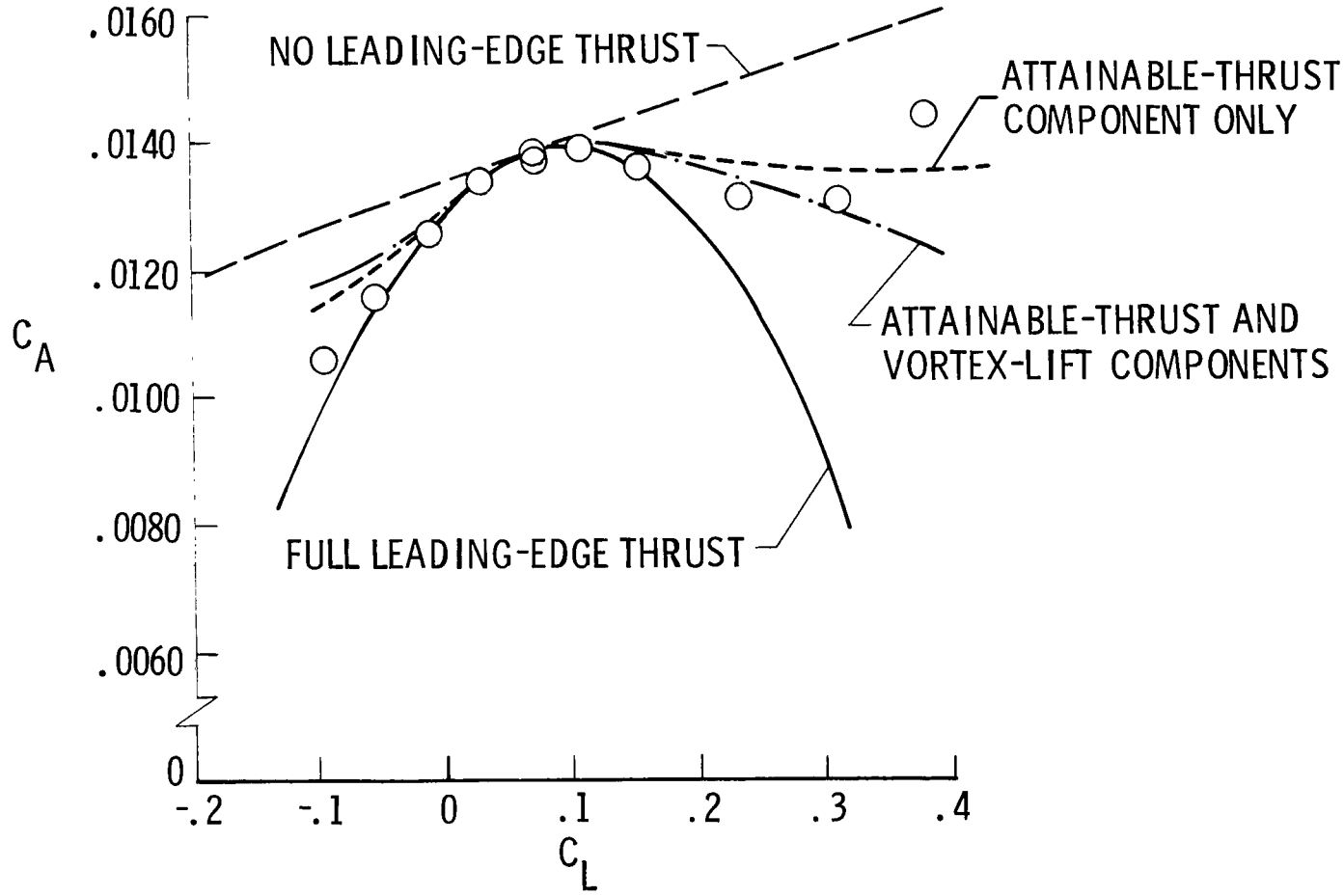

Figure 5.- Experimental and theoretical axial-force characteristics. $M = 1.8$; $R_{\bar{c}} = 2.07 \times 10^6$.

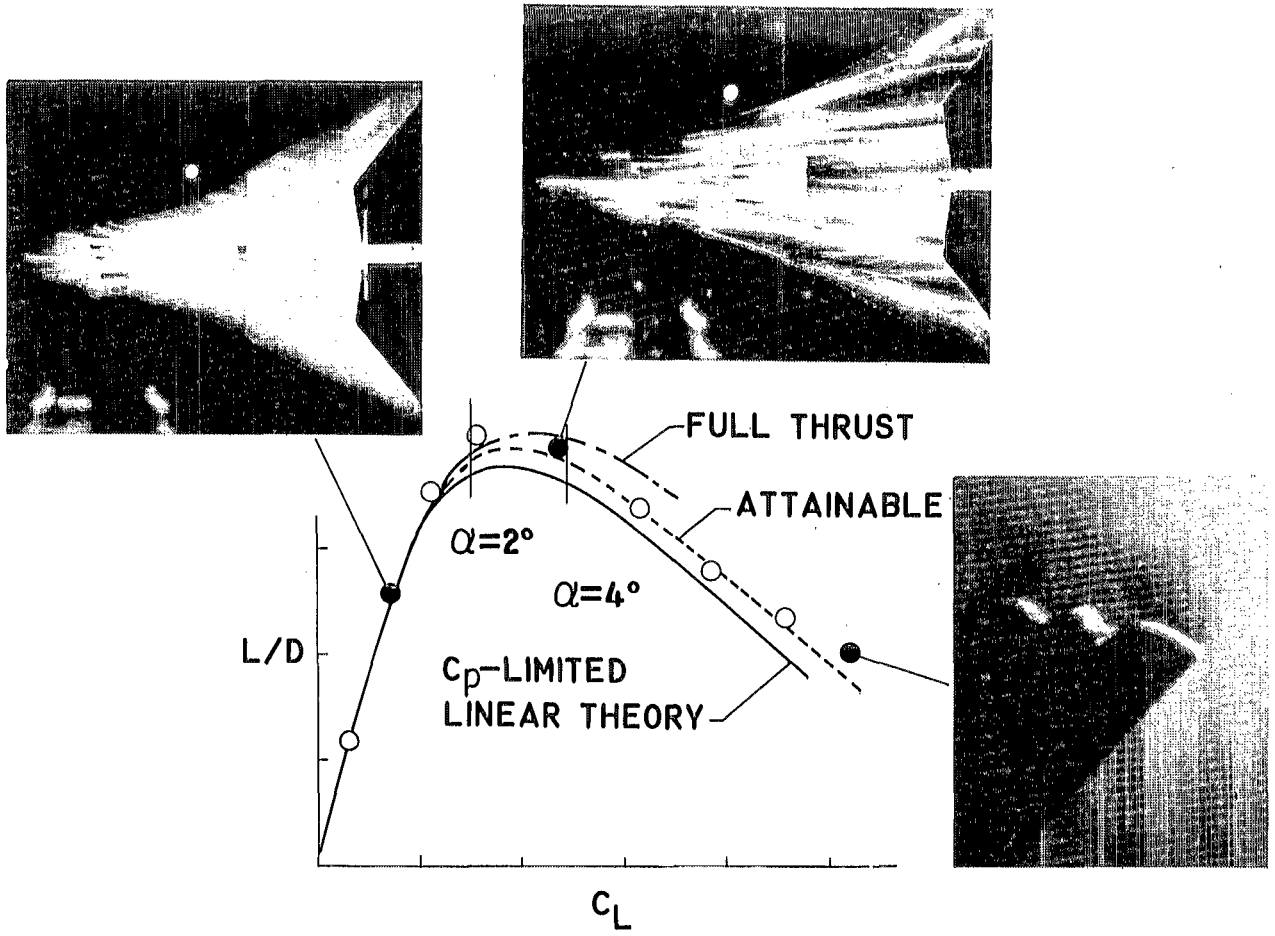

L-80-125

Figure 6.- Comparison of theories with both qualitative and quantitative experimental data.

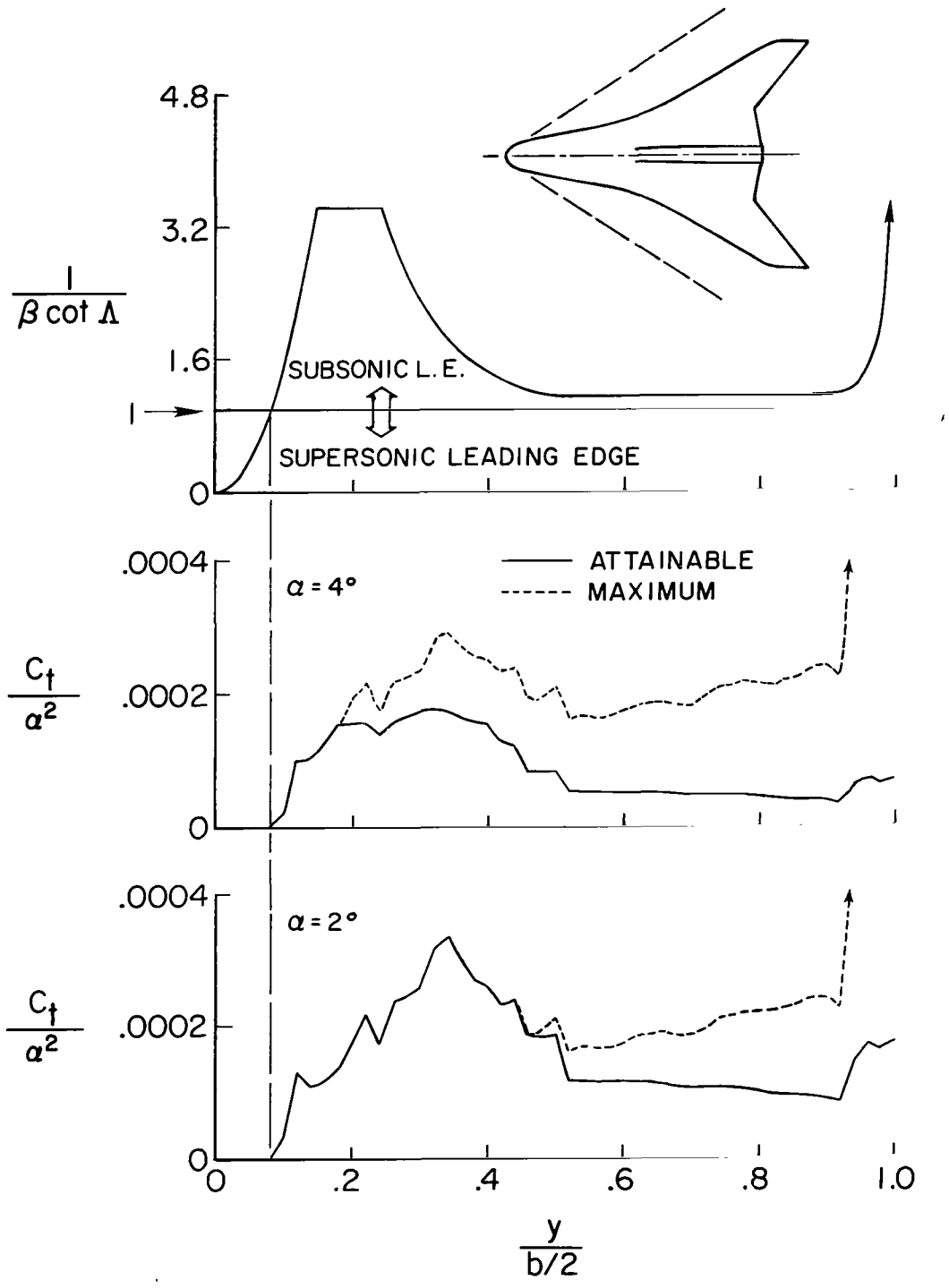

Figure 7.- Spanwise distribution of leading-edge-design and leading-edge-thrust parameters. M = 1.80; $R_{\bar{c}} = 2.07 \times 10^6$; t/c = 0.04.

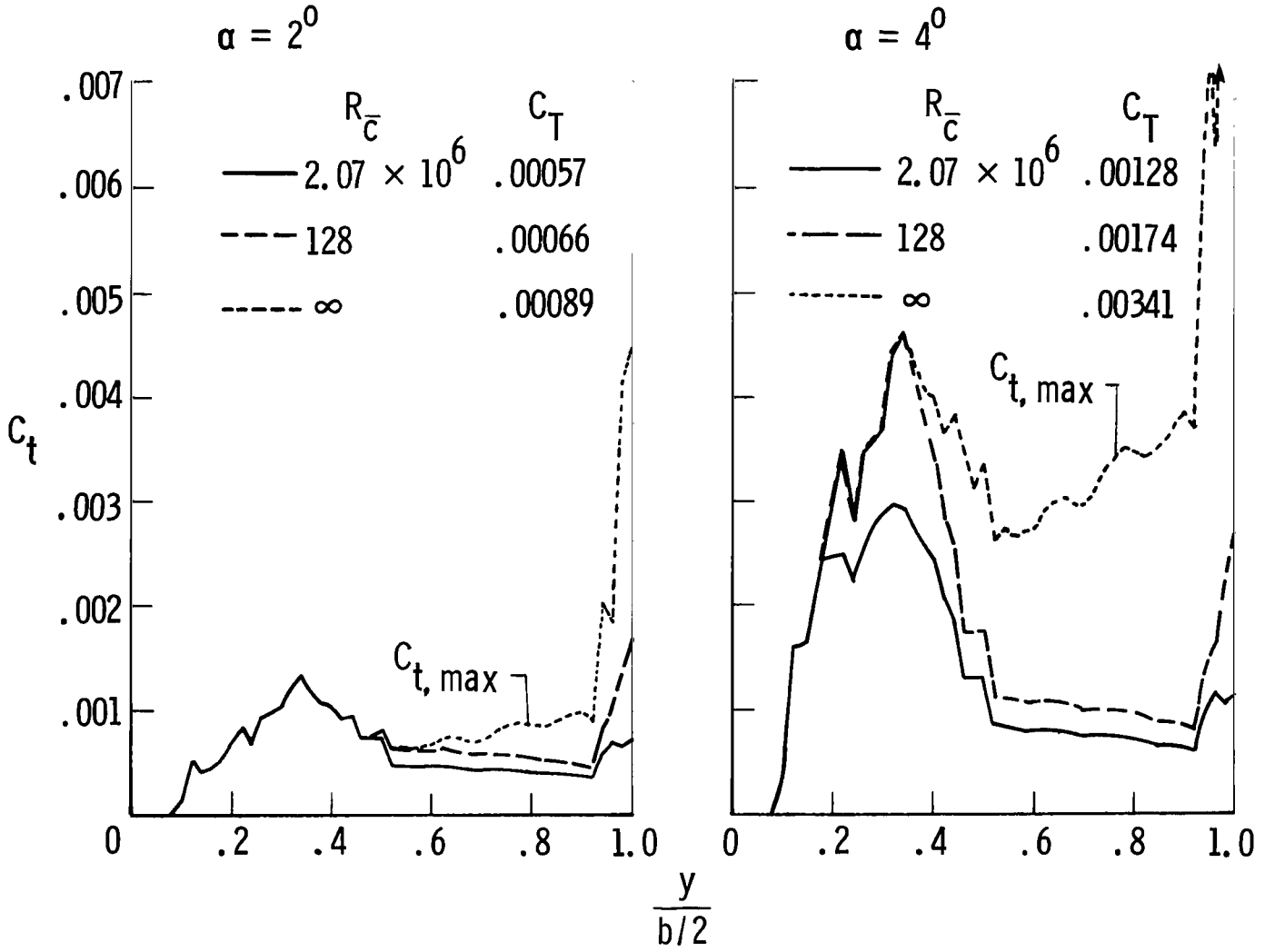

Figure 8.- Leading-edge thrust dependency on Reynolds number. M = 1.8; t/c = 0.04.

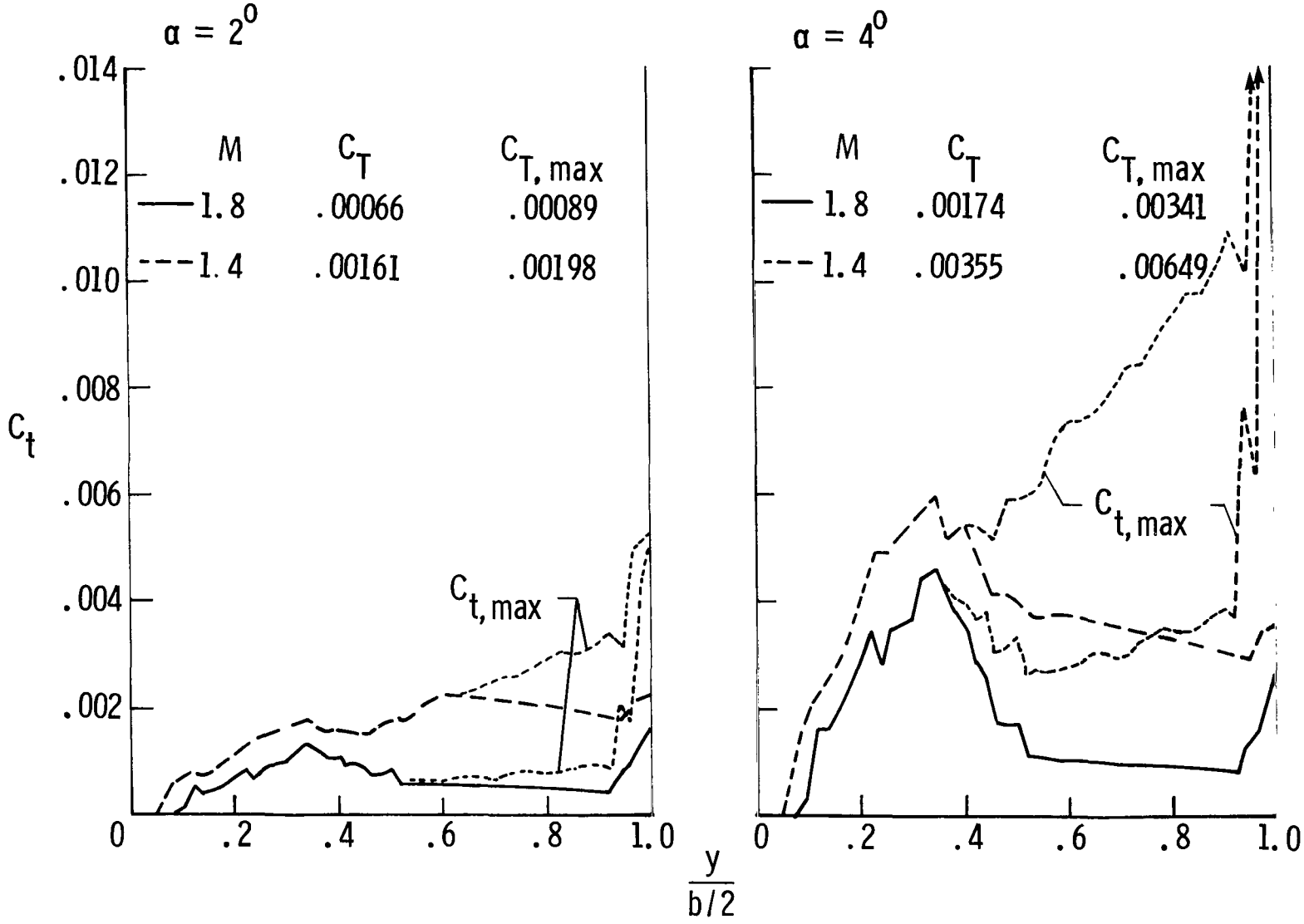

Figure 9.- Leading-edge thrust dependency on Mach number. $R_{\bar{c}} = 128 \times 10^6$; t/c = 0.04.

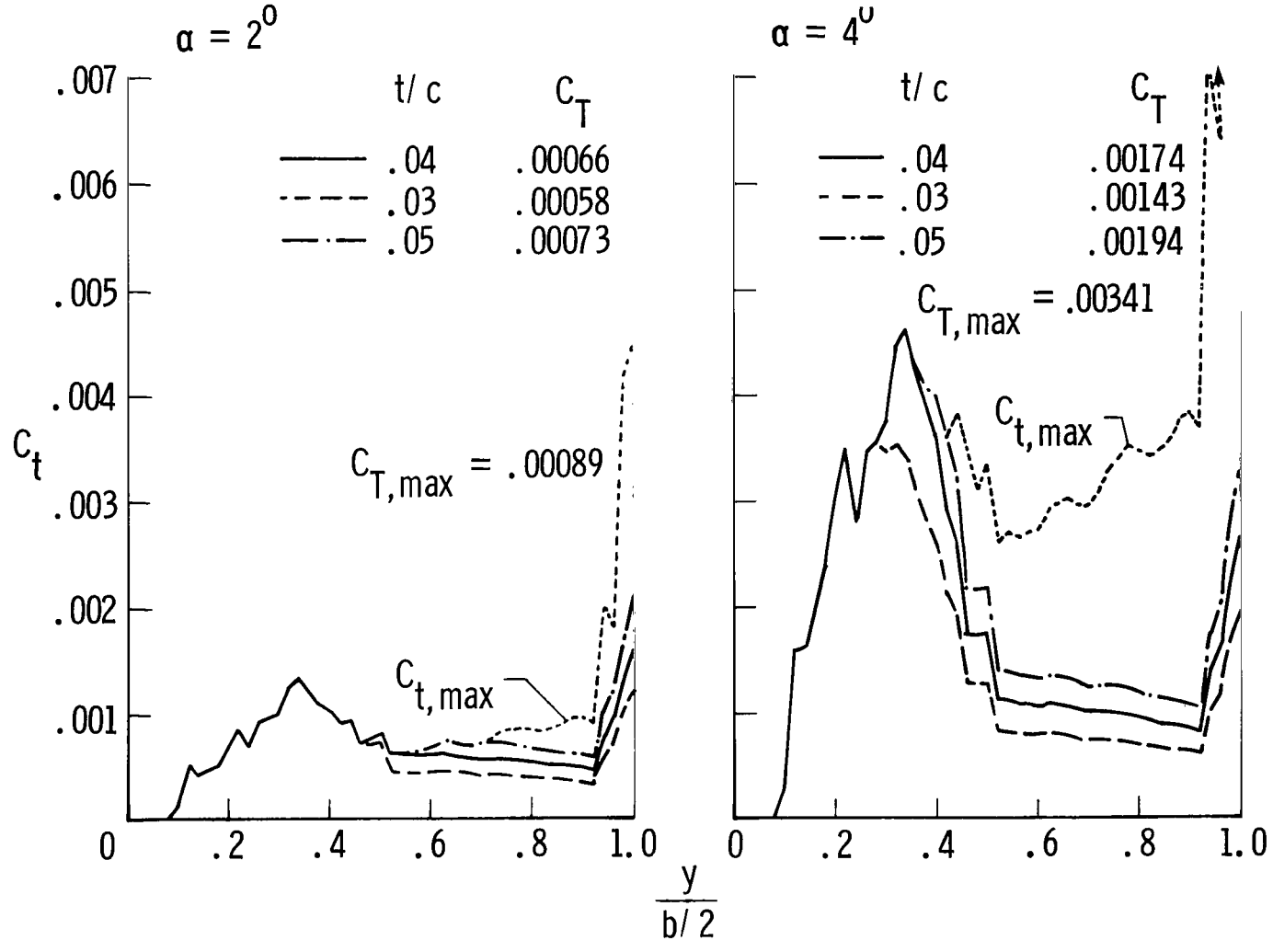

Figure 10.- Leading-edge-thrust dependency on thickness ratio. M = 1.8; $R_{\bar{c}} = 128 \times 10^6$.

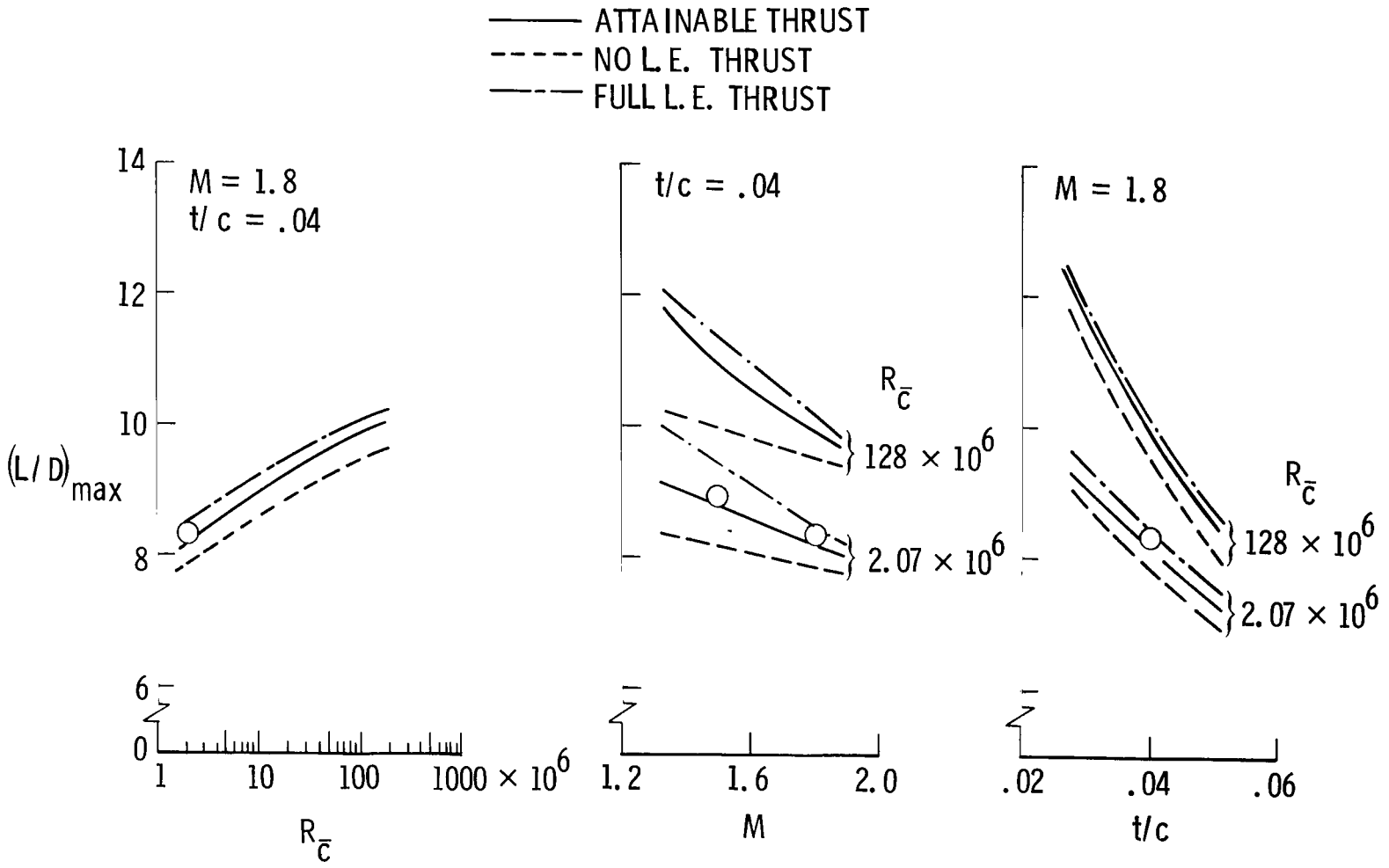

Figure 11.- Maximum lift-drag ratio as affected by Reynolds and Mach number and thickness ratio.

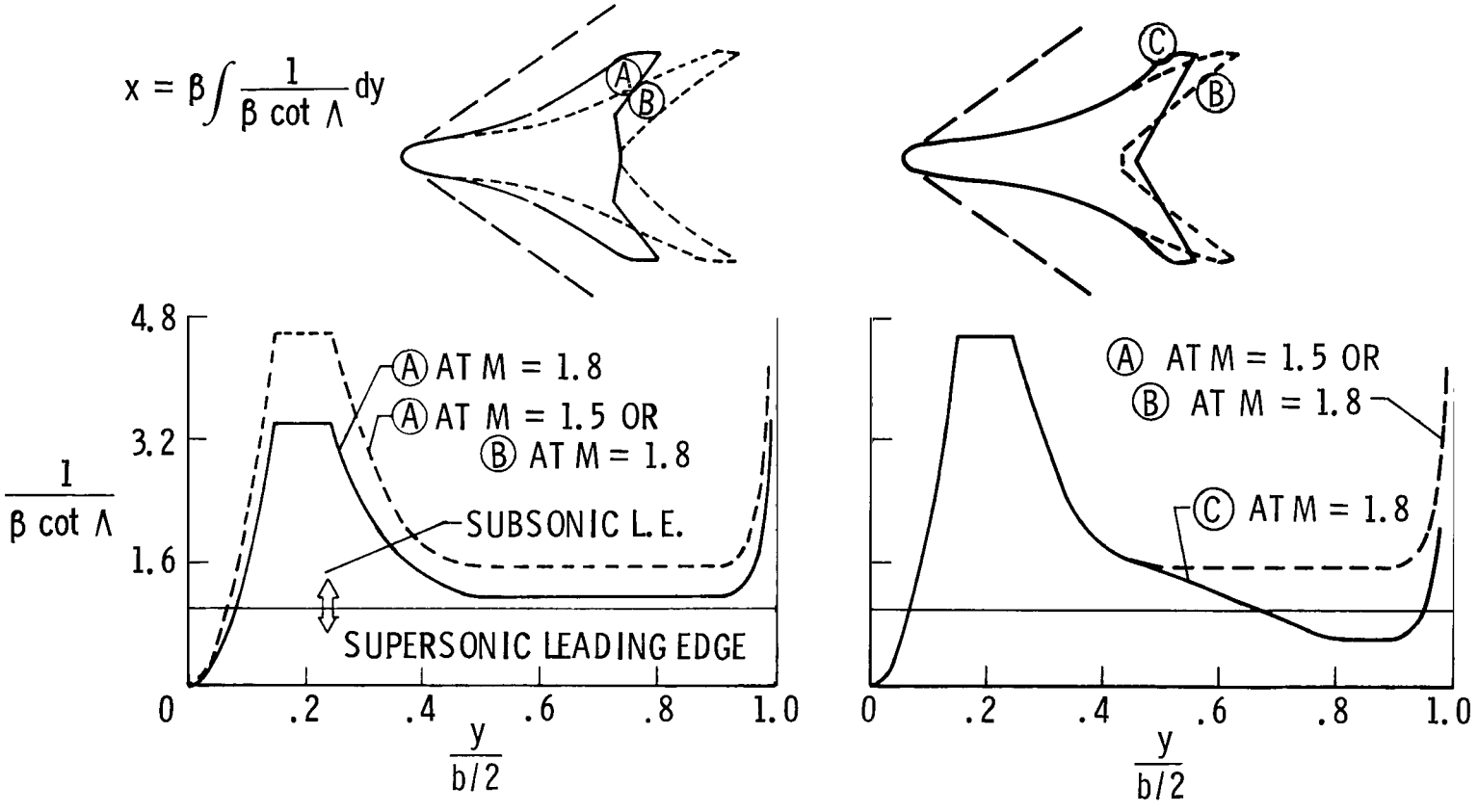

Figure 12.- Consideration of leading-edge design parameter in design of alternate wings. Ⓐ, Ⓑ, and Ⓒ represent configurations A, B, and C, respectively.

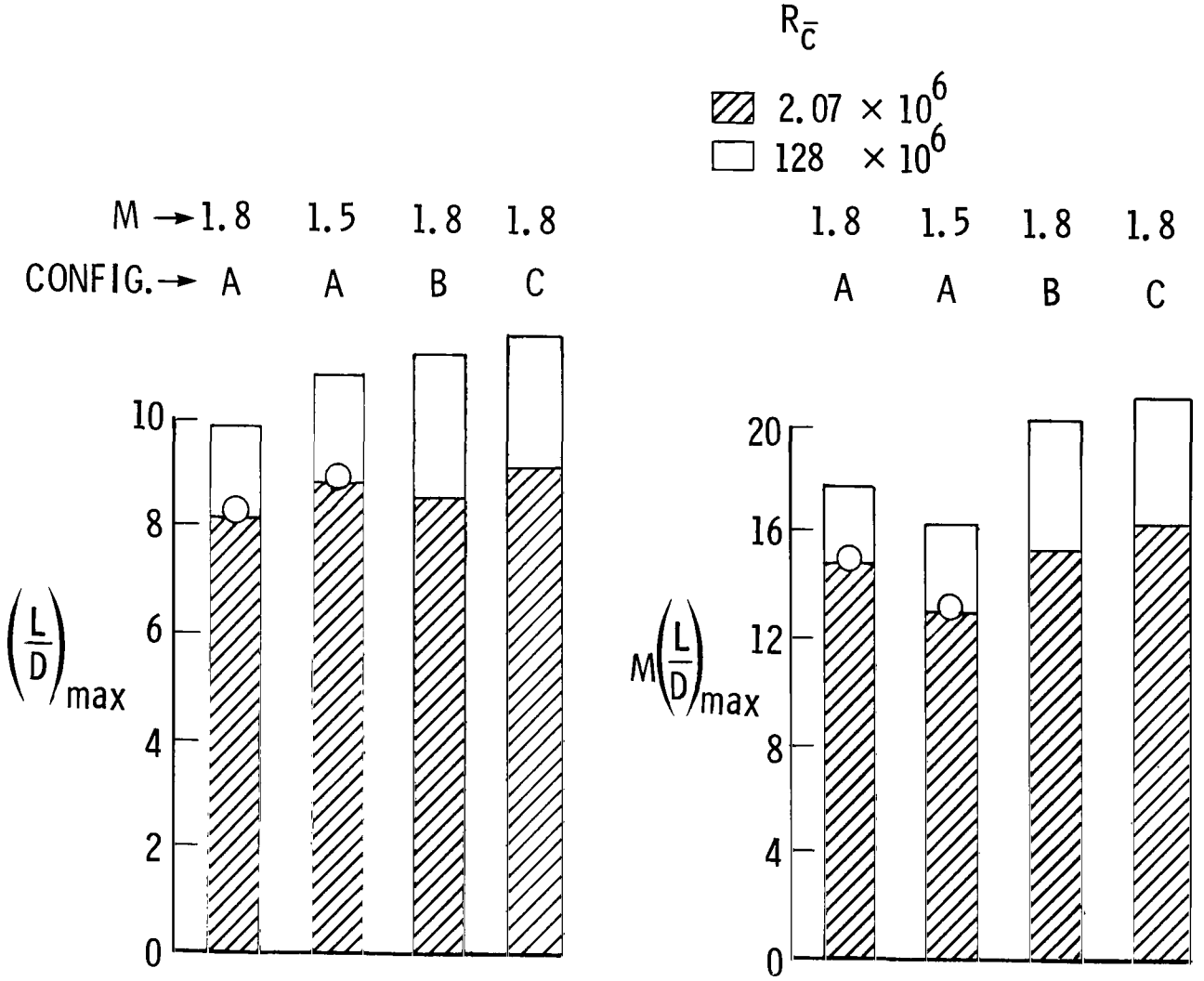

Figure 13.- Aerodynamic performance of original and alternate wings.

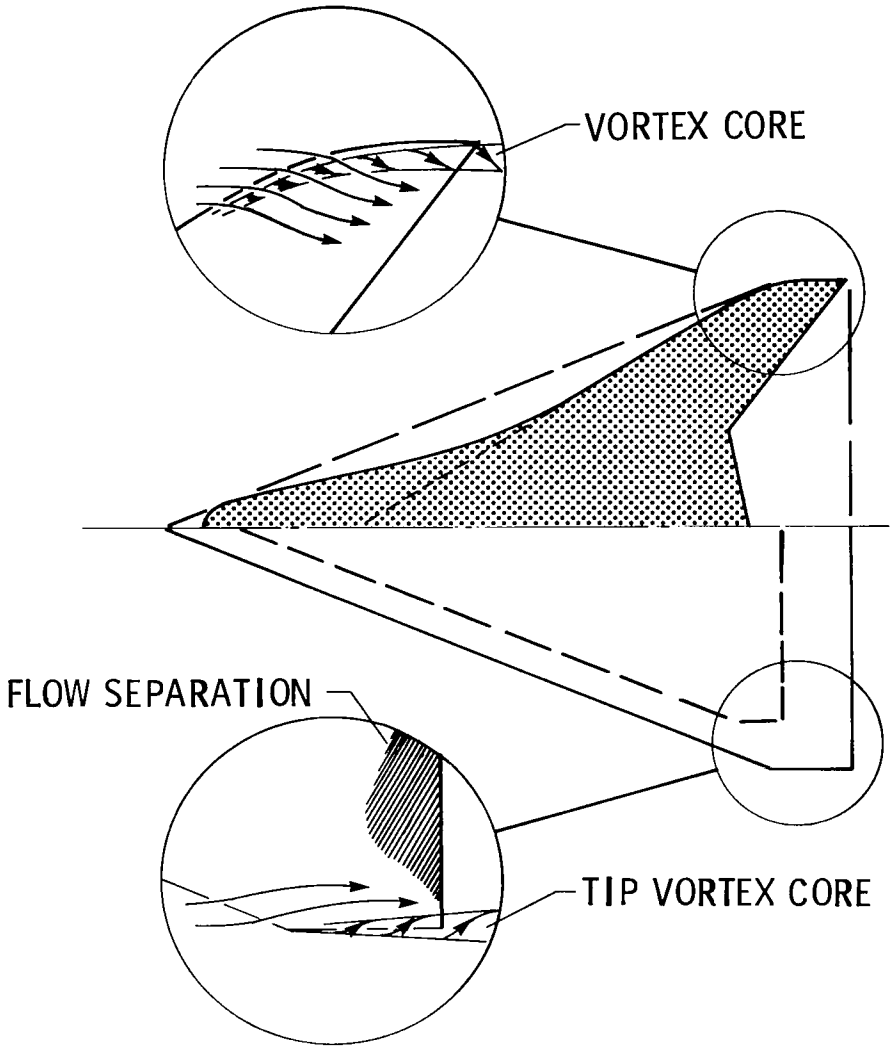

Figure 14.- Additional considerations in supersonic-wing design.

1. Report No.	2. Government Accession No.	3. Recipient's Catalog No.
NASA TP-1632		

4. Title and Subtitle	5. Report Date
SUPERSONIC WINGS WITH SIGNIFICANT LEADING-EDGE THRUST AT CRUISE	April 1980
	6. Performing Organization Code
7. Author(s)	8. Performing Organization Report No.
A. Warner Robins, Harry W. Carlson, and Robert J. Mack	L-13316
	10. Work Unit No.
9. Performing Organization Name and Address	505-31-43-01
NASA Langley Research Center Hampton, VA 23665	11. Contract or Grant No.
	13. Type of Report and Period Covered
12. Sponsoring Agency Name and Address	Technical Paper
National Aeronautics and Space Administration Washington, DC 20546	14. Sponsoring Agency Code

15. Supplementary Notes

16. Abstract

Experimental/theoretical correlations are presented which show that significant levels of leading-edge thrust are possible at supersonic speeds for certain planforms having the geometry to support the theoretical thrust-distribution potential. The new analytical process employed provides not only the level of leading-edge thrust attainable but also the spanwise distribution of both it and that component of full theoretical thrust which acts as vortex lift. Significantly improved aerodynamic performance in the moderate supersonic speed regime is indicated.

17. Key Words (Suggested by Author(s))	18. Distribution Statement
Supersonic aerodynamics Leading-edge thrust Supersonic wing design Aerodynamic performance prediction Wing planform study	Unclassified - Unlimited Subject Category 02

19. Security Classif. (of this report)	20. Security Classif. (of this page)	21. No. of Pages	22. Price*
Unclassified	Unclassified	25	$4.00

*For sale by the National Technical Information Service, Springfield, Virginia 22161

NASA-Langley, 1980